No need for merging

7 Diffraction II

7.1 Fresnel Diffraction

Let us now continue our discussion of diffraction by considering the Fresnel regime, where the aperture is much larger than the Fresnel length $r_F = (\lambda r)^{1/2}$ and there is a large phase variation over the aperture. Specialize to incoming wave vectors that are approximately orthogonal to the aperture and to small diffraction angles so that we can ignore the obliquity factor. In contrast to the Frauenhofer case, identify $\mathcal{P}$ by its distance z from the aperture plane, instead of its distance r from the aperture center, and use as integration variable in the aperture $\mathbf{x}' \equiv \mathbf{x} - r\boldsymbol{\theta}$ (see figure 1).

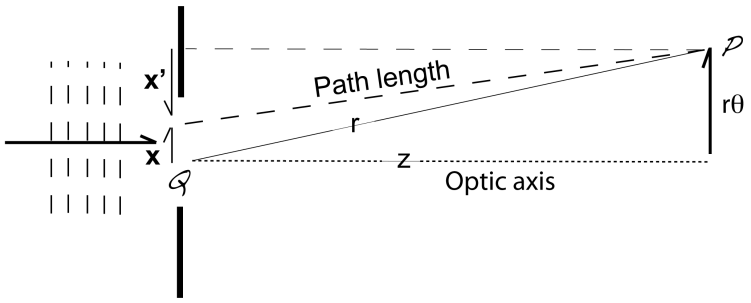

Figure 1: Geometry for computing the path length between a point $\mathcal{Q}$ in the aperture and the observation point $\mathcal{P}$. The transverse vector $\mathbf{x}$ is used to identify $\mathcal{Q}$ in the Frauenhofer analysis and $\mathbf{x}'$ is used for Fresnel analysis.

We can then write the dependence of the phase at $\mathcal{P}$ on $\mathbf{x}$ in the form

$$\Delta\phi \equiv k \times [(\text{path length from } \mathbf{x} \text{ to } \mathcal{P}) - z] = \frac{k\mathbf{x}'^2}{2z} + O\left(\frac{kx'^4}{z^3}\right)$$

Exercise

1. Why is $\Delta\phi \approx \frac{k\mathbf{x}'^2}{2z}$?

In the Fresnel regime the term quadratic in $\mathbf{x}$ is significant, and this the reason the new variable $\mathbf{x}'$ has been introduced is to simplify this expression.

As in the case of Frauenhofer diffraction, let us consider the diffraction pattern formed by a simple aperture of arbitrary shape, illuminated by a normally incident plane wave. It is convenient to use Cartesian coordinates (x', y') and to define

$$s = \left(\frac{k}{\pi z}\right)^{1/2} x', \qquad t = \left(\frac{k}{\pi z}\right)^{1/2} y'.$$

Notice that $(k/\pi z)^{1/2}$ is $\sqrt{2}/r_F$. Since we are assuming that the light is nearly orthogonal to the aperture we set the obliquity factor to one, and we can therefore rewrite (see lecture notes 5)

$$\psi_{\mathcal{P}} = -\frac{ik}{2\pi}\int_{\mathcal{Q}} d\boldsymbol{S}\cdot\left(\frac{\boldsymbol{n}+\boldsymbol{n}'}{2}\right)\frac{e^{ikr}}{r}t\psi'$$

to

$$\psi_{\mathcal{P}} = -\frac{ike^{ikz}}{2\pi z}\int_{\mathcal{Q}} e^{i\Delta\phi}\psi_{\mathcal{Q}}dx'dy' = -\frac{i}{2}\int\int e^{i\pi s^2/2}e^{i\pi t^2/2}\psi_{\mathcal{Q}}e^{ikz}dsdt.$$

Exercise

2. Check that this is correct.

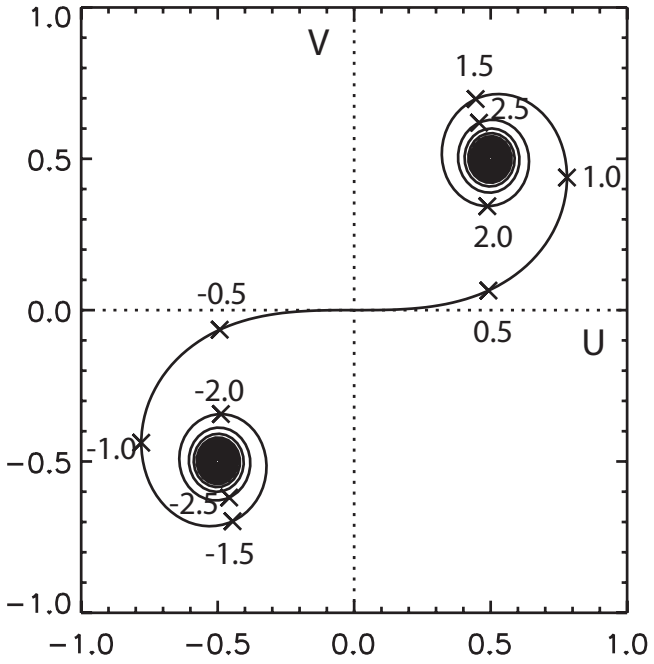

Figure 2: The Cornu Spiral showing the behaviour of the Fresnel integrals $U(\xi)$ and $V(\xi)$.

The expression above is quite general. Let us here concentrate on the Fresnel diffraction pattern for an incoming plane wave that falls perpendicularly on the aperture, so $\psi_{\mathcal{Q}}$ is constant over the aperture. Let us also confine ourselves to a rectangular aperture, with edges along the x' and y' directions. Then the two integrals have limits that are independent of each other and that can be expressed in the form $S(s_{max}) - S(s_{min})$ and $S(t_{max}) - S(t_{min})$ so

$$\psi_{\mathcal{P}} = \frac{-i}{2}[S(s_{max}) - S(s_{min})][S(t_{max}) - S(t_{min})]\psi_{\mathcal{Q}} e^{ikz} \equiv \frac{-i}{2}\Delta S_s \Delta S_t \psi_{\mathcal{Q}} e^{ikz}, \tag{1}$$

where the arguments are the limits of integration and where

$$S(\xi) \equiv \int_0^{\xi} e^{i\pi s^2/2} ds \equiv U(\xi) + iV(\xi)$$

with

$$\begin{aligned} U(\xi) &= \int_0^{\xi} ds\, \cos(\pi s^2/2) \\ V(\xi) &= \int_0^{\xi} ds\, \sin(\pi s^2/2) \end{aligned}$$

The real functions $U(\xi)$ and $V(\xi)$ are known as the *Fresnel integrals*.

The Fresnel integrals can be exhibited graphically using the *Cornu spiral*, which is a graph of the parametric equation $[U(\xi), V(\xi)]$, or equivalently a graph of $S(\xi) = U(\xi) + iV(\xi)$ in the complex plane.

The simplest illustration is the totally unobscured, plane wavefront. In this case the limits of both integrations extend from $-\infty$ to $+\infty$, which as is seen from figure 2 is an arrow of length $\sqrt{2}$ and phase $\pi/4$. Therefore, $\psi_{\mathcal{P}}$ is equal to $(2^{1/2}e^{i\pi/4})^2(-i/2)\psi_{\mathcal{Q}}e^{ikz} = \psi_{\mathcal{Q}}e^{ikz}$, as we could have seen from solving the Helmholtz equation for a plane wave.

Still following Kip Thorne's lecture notes, we make the following points

- Considering the integral derived above it is clear that only those light paths that are within a few Fresnel lengths of the geometric-optics path of least distance contribute to the wave field at the point $\mathcal{Q}$.
- Reltated to this, when computing the diffraction pattern from a more complicated aperture it is only necessary to perform the integral in the immediate vicinity of the geometric-optics ray.
- Finally, when integrating over the whole area of the wave front at $\mathcal{Q}$, we sum contributions with increasingly large phase differences that add up in such a way that the total has a net extra phase of $\pi/2$, relative the geometric optics ray. This phase factor cancels exactly the prefactor $-i$ in the Fresnel-Kirchhoff integral.

7.2 Lunar Occultation of a Radio Source

The next simplest case of Fresnel diffraction is the pattern formed by a straight edge. Let us take the example of a quasar's radio waves being occulted by the moon. Treating the lunar limb as a straight edge, the radio source will create a changing diffraction pattern as it passes behind the moon, and this

pattern can be measured by a radio telescope on the earth. Orient the coordinates such that the moons edge is along the y' (or t) direction. Then we have $\Delta S_t \equiv S(t_{max}) - S(t_{min}) = \sqrt{2i}$ is constant, and $\Delta S_s \equiv S(s_{max}) - (s_{min})$ is described by the Cornu spiral: long before the occultation, ΔS_s is given by the arrow from $(-1/2, -1/2)$ to $(1/2, 1/2)$, *i.e.* $\Delta S_s = \sqrt{2i}$, and the observed amplitude is $\psi_{\mathcal{Q}} e^{ilks}$. When the moon begins to occult the radio source, the upper bound on the Fresnel integral begins to diminish from $s_{max} = +\infty$, and the complex vector on the Cornu spiral begin to oscillate in length and phase. The observed flux will also oscillate, more and more strongly as as geometric occultation is approached. At the point of geometric occultation, the complex vector extends from $(-1/2, -1/2)$ to $(0, 0)$ and so the observed wave amplitude is one half the occulted value and the intensity is one fourth. As the occultation proceeds, the length of the complex vector and thus the observed flux will decrease monotonically to zero, while the phase continues to oscillate.

Historically, diffraction of a radio source's waves by the moon led to the discovery of quasars.

Exercise

3. Derive a formula for the intensity diffraction pattern $F(x)$ of a slit with width a, as a function of distance x from the center of the slit, in terms of Fresnel integrals.

4. Recreate figure 2 using IDL. The following fragments of code might be useful

```
function fresnel_cos,xi
;
fcos=fltarr(n_elements(xi))
for i=0,n_elements(xi)-1 do begin
  npt=10000
  s=findgen(npt)/npt*xi[i]
  fcos[i]=trapez(s,cos(!pi*s*s/2.))
endfor
return,fcos
;
end
```

   and equivalent for `fsin`, which both call the fuction

```
function trapez,x0,y0
;
n=n_elements(x0)
x=fltarr(n)+x0
y=fltarr(n)+y0
integrand=(y+shift(y,-1))*(shift(x,-1)-x)
return,total(integrand(0:n-2))*0.5
;
end
```

   (I am sure that this integral can be done in a **much** better way using calls to the error function $\mathrm{erf}(x) = \frac{2}{\sqrt{\pi}} \int_0^x e^{-t^2} dt$!, but this will work.)

5. Using IDL and the routines above, plot the one-dimensional intensity diffraction pattern $|\psi|^2$ produced by a slit, $t(x) = 1$ for $|x| < a/2$ and $t(x) = 0$ for $|x| > a/2$, for the values $r_F/a = 0.05, 0.5, 1, 2$.

7.3 Circular Apertures

The diffraction pattern for a plane wave can be thought of as formed by waves that derive from a patch a few Fresnel lengths in size. This point can be driven home by reanalyzing the unobstructed wave front in circular polar coordinates.

Consider a plane wave incident on an aperture $\mathcal{Q}$ that is infinitely large, and define $\rho \equiv |\mathbf{x}'|/r_F = \sqrt{\frac{1}{2}(s^2+t^2)}$. Then the phase factor in equation 1 is $\Delta\phi = \pi\rho^2$ and the observed wave will thus be given by

$$\begin{aligned}\psi_{\mathcal{P}} &= -i\int_0^{\rho} 2\pi\rho d\rho\, e^{i\pi\rho^2}\psi_{\mathcal{Q}}e^{ikz} \\ &= (1-e^{i\pi\rho^2})\psi_{\mathcal{Q}}e^{ikz}.\end{aligned}$$

This integral does not converge as $\rho \to \infty$! Why is that? Add up the contributions to $\psi_{\mathcal{P}}$ from each annular ring as one integrates outward from $\rho = 0$; when one has integrated out to a radius of r_F, *i.e* $\rho = 1$, the contribution to the observed wave is $\psi_{\mathcal{P}} = 2\psi_{\mathcal{Q}}$, in phase with the incident wave. But, when the integration has been extended to $\sqrt{2}r_F$, $\rho = \sqrt{2}$, $\psi_{\mathcal{P}} = 0$. And as ρ increases the integral will continue to oscillate.

Of course, we have already proven that this integral converges. Let us analyze what is going on by by splitting up the aperture $\mathcal{Q}$ into concentric annular rings, known as *Fresnel half-period zones*, of radius $\sqrt{n}r_F$, where $n = 1, 2, 3, \ldots$. The odd numbered rings cancel out the contribution from the even number rings. However, the thickness of these rings decreases as $1/\sqrt{n}$, and eventually one must allow for the fact that the incoming wave is not exactly planar, or equivalently that the wave's distant source has finite size. The finite size causes the different pieces of the source to have their Fresnel rings centered at slightly different points in the aperture plane, causing the computation of $\psi_{\mathcal{P}}$ to begin averaging over rings, and the intensity asymptotes to $|\psi_{\mathcal{Q}}|^2$.

Why have we then chosen such a strange way of decomposing a plane wave front? Because it allows for a particularly striking experimental verification of the theory of diffraction propounded here. Suppose one fabricates an aperture (a *zone plate*) in which, for a chosen observation point $\mathcal{P}$ on the optic axis, alternate half-period zones are obscured. Then the wave observed at $\mathcal{P}$ will be the linear sum of several diameters, and the sum should be larger than $\psi_{\mathcal{Q}}$. This strong amplification is confined to our chosen spot on the optic axis; most everywhere else the field's intensity is reduced, thereby conserving energy. Thus, the zone plate behaves like a lens. The lens' focal length is $f = kA/2\pi^2$, where A (typically chose to be a few mm^2 for a table top experiment) is the area of the first half-period zone. An interesting historical side note is that Poisson predicted this spot as a consequence of Fresnel's theory of light, and was planning to use it as an argument to disprove the theory. However, it was quickly demonstrated that the bright spot actually existed!

Zone plates are only good lenses when the radiation is monochromatic, since the focal length is wavelength-dependent $f \propto \lambda^{-1}$. Further, they have the interesting property that they posses secondary foci, where the fields from $3, 5, 7, \ldots$

contiguous zones add up coherently.

Exercises

6. Explain why the focal length of a zone plate is $f = kA/2\pi^2$.

7. An opaque, perfectly circular disk of diameter D is placed perpendicular to an incoming plane wave. Show that, at distances r such that $r_F \ll D$, the disk casts a rather sharp shadow, but at the precise center of the shadow there should be a bright spot. How bright?

7.4 Seeing in the atmosphere

7.4.1 A simple model (with exercises)

Stars viewed through the atmosphere appear to have angular diameters of order an arc second and to exhibit large amplitude fluctuations of flux with characteristic frequencies that can be as high as 100 Hz. Both of these phenomena are a consequence of irregular variations in the refractive index of the atmosphere. A simple model of this effect consists of a thin phase-changing screen, about a km above the ground, on which the rms phase variation is $\Delta\phi \gtrsim 1$ and the characteristic spatial scale on which the scale changes by $\sim \Delta\phi$ is a.

It is straightforward to show that rays will be irregularly deflected through a scattering angle $\Delta\theta \sim (\lambda/a)\Delta\phi$. Strong intensity variations require that several rays deriving from points on the the screen separated by more than a, combine at each point on the ground. These rays combine to create a diffraction pattern on the ground with scale b.

It is possible to show that the Fresnel length in the screen is $\sim \sqrt{ab}$. The time variation in the observed intensity arises because winds in the upper atmosphere with speeds $u \sim 30\ \mathrm{m\,s^{-1}}$ blow the irregularities and the diffraction pattern past the observer. The information given above is sufficient to estimate the Fresnel length r_F, the atmospheric fluctuation scale size a, and the rms phase variation $\Delta\phi$.

Exercises

8. Explain why $\Delta\theta \sim (\lambda/a)\Delta\phi$.

9. Show that the Fresnel length in the screen is $\sim \sqrt{ab}$.

10. Use the information given above to estimate r_F, the atmospheric fluctuation scale a, and the rms phase variation $\Delta\phi$.

7.4.2 Effects of the atomsphere (including better model)

The two major effects of the Earth's atmosphere are *atmospheric refraction* and distorted wavefronts (or *seeing*) due to refraction in a turbulent atmosphere.

We can approximate the atmosphere as a series of plane-parallel plates, and the surface as an infinite plane. A ray incindent at angle α refracts at each of the interfaces, and will ultimately make a new angle $\alpha + \Delta\alpha$ with the surface: thus, refraction shifts the apparent position of the source towards the zenith. The atmosphere consists of a very large number of thin layers and the total effect of refraction is to curve the path of the incident ray. In this limit Fermat's principle and the plane-parallel model gives

$$\Delta\alpha = R_0 \tan\alpha = \frac{n^2 - 1}{2n^2} \tan\alpha \approx (n-1)\tan\alpha$$

where n is the index of refraction at the surface. The quantity $(n-1) \times 10^6$ is the *refractivity*. Since the index is a function of wavelength rays of different colors are refracted at different angles, and at large zenith distances images are actually very low resolution spectra — with the blue image shifted more towards the zenith than red.

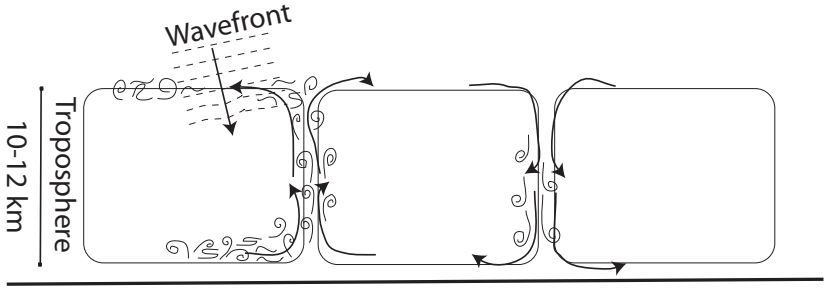

Figure 3: Sketch of atmospheric circulation in the troposphere and the effects it has on incoming wavefronts. Locally heated air near the ground will become boyant and rise, resulting in a convective flow as cool air flows to fill its place. Turbulence is enhanced at the boundaries of convection cells.

In a perfectly serene and quiet atmosphere, then density and index of refraction of air will depend only on altitude, and every point at the same height will have the same index. In the real atmosphere solar heating drives convective cells in the lowest layer of the atmosphere, a region some 10–12 km thick called the *troposphere*. One mass of air can become slightly hotter and more bouyant than its neighbors and therefore rise. Another mass moves horizontally to take its place; cold air from above drops down to make room for the rising mass and completes the circulation around a cell. Many cells are established, and the air, especially at the boundaries of the flow, tends to break up into turbulent eddies of different density and temperature.

A wavefront from a distant star passing through the atmosphere arrives as a plane, but different parts will encounter slightly different patterns in the index of refraction. Each ray will traverse slightly different optical path, and the wavefront will no longer be a plane. Since the turbulent eddies at each

altitude move at the local wind speed, the distortion in the wavefront changes very quickly.

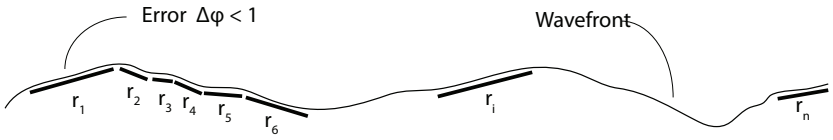

Figure 4: Quantifying the wavefront is done by fitting the wavefront with straight segments along which the difference between vertical z direction between the fit and the wavefront is less than $\lambda/2\pi$ (equivalent to changes in phase $\Delta\phi < 1$). The length of a segment r_i is called the coherence length and the average of all segments is the coherence length of the wavefront.

We can quantify this wavefront distortion. Consider first a one-dimensional model, start at one end of the wavefront and fit a straight line to a segment of the front. How long can this segment be before the fit becomes "poor"? We need a criterion for judging the goodness of fit, and we choose the root mean square (RMS) difference in the vertical z direction between the front and the fit. If this quantity becomes greater than $\lambda/2\pi n$, then fit is poor. This is equivalent that the RMS deviation of phase ϕ is less than one radian. The maximum length that can be fit is r_1, called the coherence length of the first segment. Moves along the front fitting successive segments of "good fit" r_i. The statistical mean of all the r_i values is $r_{\rm avg}$ the *coherence length of the wavefront*. Each segment has a different slope, so each will propagate in a slightly different direction, and each will focus at a different spot in the image plane of a telescope. The shorter the coherence length, the more *speckles* in the image.

Extending to two dimensions: select a random point on a two-dimensional wavefront and ask how large a 2D patch of the front we can expect to be choherent. The answer is called *Fried's parameter* $r_{0\lambda}$, the expected diameter over which the RMS optical phase distortion is 1 radian.

7.4.3 Real time atmospheric compensation

Arguments of the sort given above (though with a somewhat more sophisticated model of atmospheric turbulence) can be used to derive the maximum diameter of a telescope before it becomes seriously affected by *seeing*, given by Fried's coherence length

$$r_0 \approx 0.114 \left(\frac{\lambda \cos z}{550} \right)^{0.6} \text{ m}$$

where λ is the observing wavelength in nm and z is the zenith angle. Fried's coherence length, r_0 is the distance over which the phase difference is one radian, and plays the same role as a in the simpler model above. In particular, the full

width at half maximum of the seeing disk is given by

$$\theta \approx 0.2 \frac{\lambda[\mu\mathrm{m}]}{r_{0\lambda}[\mathrm{m}]}$$

If the diameter of a telescope, D, is larger than $r_{0\lambda}$, then this expression gives the image size. If $D < r_{0\lambda}$ the telescope is diffraction limited. Values for r_0 vary from a few centimeters to 15 or 20 cm (which is excellent seeing).

Short of placing telescopes in space above the atmosphere, one alternative is to correct the distortions introduced by atmospheric turbulence by the use of adaptive optics. In such systems, one or more of the optical components can be changed rapidly in such a manner that the undesired distortions in the light beam are reduced or eliminated.

The efficiency of an adaptive optics system is measured by the *Strehl ratio.* This quantity is the ratio of the intensity at the center of the corrected image to that at the center of ta perfect diffraction limited image of the same source. The *normalized Strehl ratio* is the Strehl ratio of the corrected image divided by that for the uncorrected ratio. Strehl ratios of up to 0.6 are currently being achieved and one may reach 0.8 in the near future.

Note that a weakness of adaptive optics is that in the visual and near infrared, the correction only extends over a very small area (the *isoplanatic patch*).

Note also that there is some confusion in the literature between terms adaptive optics and active optics. We will consider adaptive optics to be those characterised by a fast closed-loop system, and active optics a more slowly operating open- or closed-loop system. The division is made at at a response time of a few seconds. Thus, the tracking of a star by the telescope can be considered an active optics system that is open-loop if no guiding is used, and closed-loop if guiding is used. Large thin mirror optical systems may suffer distortions due to buffeting by wind at a frequency of 0.1 Hz or so; they may also distort under gravitational loading or thermal stresses. Correction of these sorts of effects also goes under the heading active optics.

An atmospheric compensation system contains three main components, a sampling system, a wave front sensor, and a correcting system.

Sampling systems. The sampling system provides the sensor with the distorted wave front or a simulacrum thereof. A beam splitter is commonly used. This is a partially reflecting mirror that typically diverts about 10% of the radiation to the sensor, while allowing the remaining 90% to continue on to form the image.

In night time astronomy even the loss of 10% of the light is to be regretted. Many adaptive systems therefore use a guide star rather than the object of interest to measure the wave front. This becomes especially important when the object to be imaged is a large extended object, since sensors generally must be used on point or near point images (or at least images with sharp gradients, see figure 6). The guide star must be very near in the sky to the object of interest or its wave front will have gone through different atmospheric distortion. The isoplanatic patch is defined by the distance over which the Strehl ratio improvement due to the adaptive optics halves. In the visible it is typically

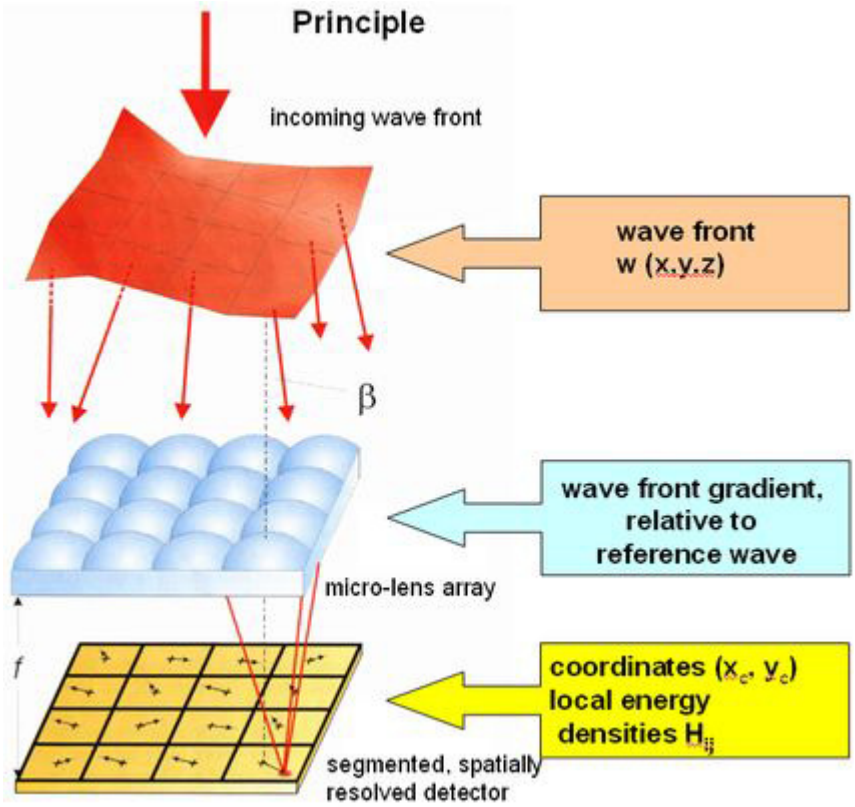

Figure 5: Prinicple of the Shack-Hartmann sensor. (figure from *Institut für Photoniche Technologien e. V.)*

of order 15 arcsec. The size of this patch scales as $\lambda^{1.2}$, so it is larger in the infrared, reaching typically 80 arcsec at 2.2 μm.

The small size of the isoplanatic patch means that few objects have suitable guide stars; less than 1% of the the sky can be covered using real stars as guides. Recently therefore, artificial guide stars have been produced. This is done by using lasers pointed skywards. The laser is tuned to one of the sodium (Na) D line frequencies and excites the free sodium atoms in the atmosphere at a height of about 90 km. The glowing atoms appear as star-like patches that can be placed as near in the sky to the object of interest as required. Guide stars at lower altitudes and at other wavelengths can be produced through back scattering by air molecules of a laser beam. Two difficulties with this technique are the *cone problem* due the geometry of the laser setup compared with the telescope and the fact that the laser light also must pass *up* through the atmosphere and therefore the guide star moves with respect to the object. Use of real stars to separately compensate tip-tilt, and the use of two or several

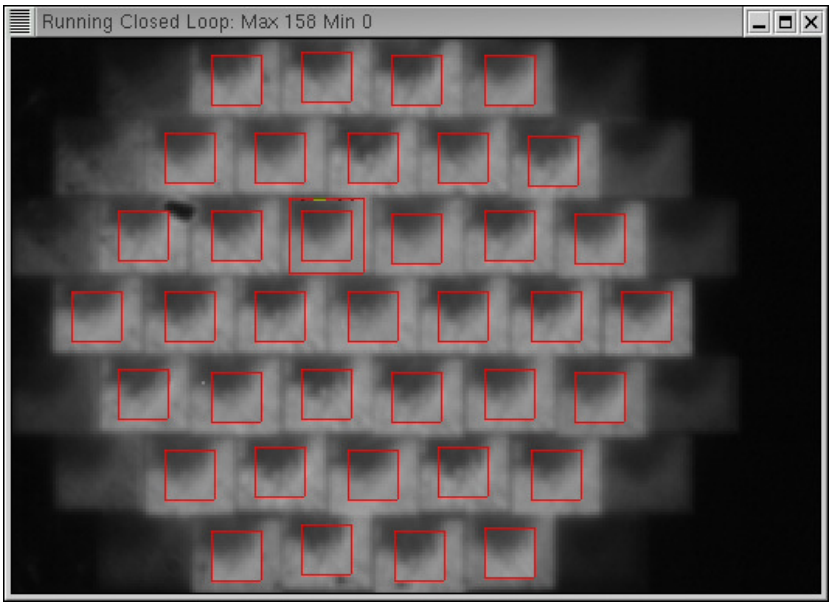

Figure 6: The multiple images of the Shack-Hartmann micro lenses as seen in the Swedish 1 meter Solar Telescope.

guide stars can eliminate some or parts of this problem.
Wave front sensing. The wave front sensor detects the residual and changing distortions in the wave front provided by the sampler after reflection from the correcting mirror. The Shack-Hartmann sensor is a two dimensional array of small lenses (figure 5). Each lens produces an image that is sensed by an array detector. In the absence of wave front distortions, each image will be centered on each detector. Distortion will displace the images from the centers of the detectors, and the degree of displacement and its direction is used to generate the error signal.
Wave front correction. The correction of the wave front is achieved by distorting a subsidiary mirror. Since the atmosphere changes on a time scale of 10 ms or so, the sampling, sensing and correction have to occur in 1 ms or less. In the simplest systems only the tip and tilt of the wave front introduced by the atmosphere is corrected. That is accomplished by suitably inclining a plane or segmented mirror placed in the light beam from the telescope in the opposite direction.

More sophisticated approaches provide better corrections; either just of the relative displacements within the distorted wave front, or of both displacement and fine scale tilt. Displacement correction typically uses a thin mirror capable of being distorted by up to 100 piezo-electric or other actuators placed underneath. The error signal from the sensor is used to distort the mirror in the opposite manner to the distortions in the incoming wave front. The reflected

wave front is therefore almost flat.

Plans for future 50 m and 100 m telescopes include adaptive secondary or tertiary mirrors up to 8 m in diameter, requiring up to 500 000 actuators to compensate the atmospheric distortions of the wave front.